

# ANALYSIS OF THE EFFECT OF FERRITE TILE GAP ON EMC CHAMBER HAVING FERRITE ABSORBER WALLS

Kefeng Liu  
EMC TEST SYSTEMS, L. P.  
2205 Kramer Lane  
Austin, TX 78758

**Abstract**—It has been known that air gaps between ferrite tiles degrade the absorbing performance of the tile absorber wall installation. However, analysis of the effect has not been thoroughly well published. This paper presents two techniques to analyze gaps between ferrite tiles. A simplified magnetic circuit method is introduced to calculate the effective permeability of the tile wall with gaps. Then, a two-dimensional Finite Element Method is used to analyze the same gap model to validate the simplified formula. The air gap formula is then incorporated into characterizing ferrite tile absorber with or without dielectric absorber as its matching element. The fully characterized ferrite absorbers can then be used to design EMC chambers. Design examples are presented to demonstrate the correlation between calculated and measured Normalized Site Attenuations for 10m/3m EMC semi-anechoic chambers.

## INTRODUCTION

EMC measurements of electronic equipment using shielded semi-anechoic chambers are becoming more and more popular during past two decades owing to its advantages over Open Area Test Sites (OATS) due to inherent site efficiency and immunity to weather conditions. Since the indoor EMC chamber simulates the OATS test environment in a shielded enclosure, reflections from the walls of the shielded enclosure must be effectively suppressed. Moreover, FCC and European standards require that the radiated emission of unintentional sources are to be measured from as low as 30 MHz, shielded EMC chambers must also provide acceptable measurement accuracy at the same low frequency range. Frequently, it is a technical challenge for shielded chambers to provide very good EMC measurement correlation to OATS at the low end of the frequency range (30 to 100 MHz). The focus of the problem is the absorbing performance of RF absorbers on the metallic surface at low frequency range. RF absorbers for EMC

applications in shielded semi-anechoic chambers can be classified into three types: electrical (dielectric) absorbers, magnetic absorbers (ferrite tiles), and hybrid absorbers (combination of ferrite tile foam absorbers).

(i). **Dielectric Absorbers**—Dielectric absorbers are typically made of carbon loaded polyurethane foam constructed in pyramidal shapes. The electromagnetic wave absorbing properties of these absorbers is derived from the lossy part of complex permittivity ( $\epsilon_r$ ) resulting from the carbon loading of the polyurethane foam. The dielectric absorber dissipates only the electric energy of the merging electromagnetic wave. To maximize the absorbing capability, the dielectric absorbing media should be located in the region where the electrical energy is a significant portion of the total field energy. With a metallic backing surface, the electric field energy is nullified on the metallic surface, and maximized at a quarter wavelength away from the metallic surfaces. Due to this fundamental limitation, dielectric absorbers for EMC applications with good performance are always designed with length in the proximity of at least a quarter of the wavelength at its lowest operating frequency[1]. Eight foot deep dielectric absorbers are very common for EMC chambers which operate to as low as 30 MHz.

In addition to the depth requirement, the carbon density loading of the foam, and the shape of the pyramidal construction also contribute to the enhancement of the performance of the absorbers. In the past, flat top and/or holly pyramid designs have been investigated. In addition, twisted pyramid design was also introduced to construct the absorber element. While, twisted pyramids are mechanically robust for installation, their absorbing performance is inferior to pyramidal absorbers constructed to the same depth.

(ii). **Magnetic Absorbers**-Magnetic absorbers fully utilize the advantage of the metallic surface on the shielded wall since the magnetic field energy is maximized on the surface. By placing the magnetic absorber on the metallic surface, absorbing properties of the magnetic absorber will perform at its maximum capability. With proper design, magnetic absorbers have very good normal incident absorbing property at as low as 30 MHz with as thin as a few millimeters in height compared to dielectric absorbers of about 2.4 meter or more for the same performance.

Three different types of magnetic absorbers are commercially available: flat ferrite tile, grid ferrite tile, and silicon rubber based sheets. Both flat and grid ferrite tiles are soft ferrite materials. The key ingredient of soft ferrite is nickel zinc ferromagnetic compound. The low frequency absorption of the soft ferrite loss is obtained by using ceramic technology for both high permeability and high loss tangent. The permeability and loss tangent are the key parameters to the performance of the ferrite tile absorber. With proper design, both flat and grid ferrite tiles can achieve reasonable absorbing performance between 30 and 1000 MHz. However, due to their high permeability, the absorbing property of both ferrite tiles is very sensitive to the air gaps between tiles[2,3].

Silicon rubber based magnetic sheet absorbers normally do not have permeability and loss tangent as high as ferrite tiles. They are normally fabricated as weather-proof narrow-band microwave absorbers. Sometimes, they are also incorporated with ferrite tiles as tuning elements to extend the frequency range.

Magnetic absorbers are usually manufactured as thin flat layers and tuned to a defined frequency band. Compared to dielectric absorbers, they are much more compact in depth and especially effective at low frequency range.

### (iii). Hybrid Absorbers

Hybrid absorbers are combinations of ferrite tile and dielectric absorbers. They are designed to

combine the advantages of both dielectric and ferrite tile absorbers. The ideal hybrid absorber performance relay would allow ferrite tile to absorb the incident RF energy at low frequencies (between 30 and 100 MHz) and dielectric absorber to take over the absorption above 100 MHz (up to 40 GHz). In reality, since the magnetic and dielectric absorbers are too dissimilar in wave impedance, such a relay of absorbing performance is very difficult to design. If the complex permittivity of the dielectric absorber is not designed properly, it is possible that a catastrophic loss of performance of both types of absorber may occur at the low frequency. To avoid this cancellation of performance, it is necessary to have a low lossy loading of the foam absorber. This condition makes the hybrid absorber design very delicate at the frequency range of 30 to 120 MHz.

The air gap effects on the absorbing performance of the ferrite tile related absorbers (including the hybrid absorbers) will be the focus of this paper. The performance of the absorber and EMC chamber performance will also be discussed

### ANALYSIS

Fig 1 shows a typical geometry of the ferrite tile absorber mounted on the shielded wall. The absorbing performance of the ferrite tile can be expressed as

$$\Gamma = \frac{E_r}{E_i} = \frac{\eta_t - \eta_o}{\eta_t + \eta_o} \quad (1)$$

where  $\Gamma$  is the reflection coefficient;  $\eta_o$  is the free-space wave impedance; and  $\eta_t$  is the wave impedance of the ferrite tile wall, which can be further expressed as:

$$\eta_t = \eta_o \sqrt{\frac{\mu_r}{\epsilon_r}} \tanh\left(\frac{2\pi t}{\lambda_o} \sqrt{\mu_r \epsilon_r}\right) \quad (1a)$$

where  $\mu_r$  and  $\epsilon_r$  are complex relative permeability and permittivity, respectively;  $t$  is the thickness of the ferrite tile; and  $\lambda_o$  is the free-space wavelength. At about 30 MHz, since the

thickness of the tile is much smaller than the wavelength, therefore

$$\tanh\left(\frac{2\pi t}{\lambda_o} \sqrt{\mu_r \epsilon_r}\right) \rightarrow j \frac{2\pi t}{\lambda_o} \sqrt{\mu_r \epsilon_r} \quad (1b)$$

Thus the wave impedance of the ferrite tile wall can be expressed as

$$\eta_t \approx j \eta_o \mu_r \frac{2\pi t}{\lambda_o} \quad (1c)$$

In (1c), one can notice that the wave impedance of the ferrite tile is independent of complex permittivity at low frequency where (1b) is valid.

Substituting (1c) into (1), and using  $\mu_r = \mu_r'' - j\mu_r'$ , equation (1) can be further expressed as

$$\Gamma = \frac{\left(\frac{2\pi t}{\lambda_o} \mu_r'' - 1\right) + j \frac{2\pi t}{\lambda_o} \mu_r'}{\left(\frac{2\pi t}{\lambda_o} \mu_r'' + 1\right) + j \frac{2\pi t}{\lambda_o} \mu_r'} \quad (2)$$

Since the thickness of the tile are designed so that at the tuning frequency near the low end (i.e. 30 MHz)

MHz)  $\frac{2\pi t}{\lambda_o} \mu_r'' \rightarrow 1$ , it can be shown that the

reflectivity can be empirically expressed as

$$R = 20 \log_{10}(\Gamma) \approx -20 \log_{10}\left(\frac{2\mu_r''}{\mu_r'}\right) \quad (3)$$

Equation (3) describes a very simple relation between the normal incident reflectivity performance of the ferrite tile absorber and the loss tangent of the intrinsic permeability. It also helps to find ways to improve the performance of the ferrite tile absorber by increasing the loss tangent of the intrinsic permeability. Fig.2 shows the complex permeability of one of the commercial ferrite tile absorbers. The permittivity of the compound is approximately equal to 11. Fig. 3 shows the comparison of reflectivity performances using (1) and (3). As demonstrated, equation (3) provides very good approximation below 50 MHz and remains valid up to about 100

MHz. Above 100 MHz, the complex permittivity of the ferrite tile starts to impact the validity of (1b). If  $\epsilon_r$  can be kept close to unity, the validity of (3) can be further extended.

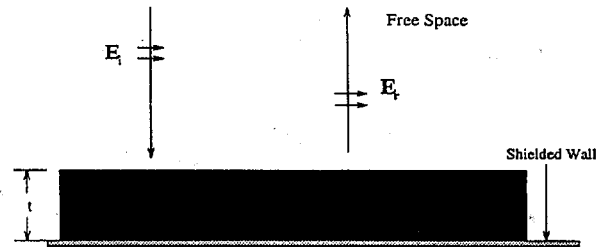


Fig.1. Ferrite tile mounted on the metallic surface

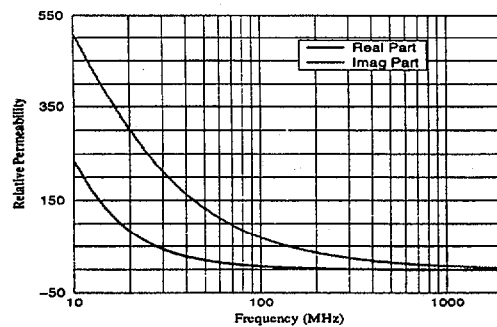


Fig. 2. Typical relative permeability of ferrite tile

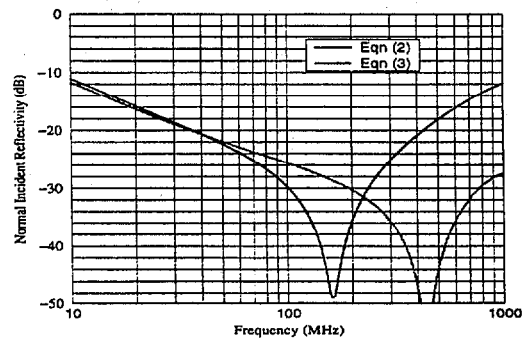


Fig. 3. Comparison of equations (1) and (3).

(a) **Gap Effects**-Since the permeability of the ferrite tiles is much larger than unity, the effect of air gaps between ferrite tile on the absorbing performance can be very serious. Such an impact is analogous to the effect of air gap in the soft iron core of the AC power transformer.

To provide a quantified analysis, the transformer core air gap formula based on magnetic circuitry theory is introduced to calculate the effective permeability of the tile wall with air gaps:

$$\mu_r^e = \frac{\mu_r}{1 + \frac{\Delta}{\ell}(\mu_r - \mu_{air})} \quad (4)$$

where  $\Delta$  is the dimension of air gap perpendicular to the magnetic field line;  $\ell$  is the width of the ferrite tile. To validate equation (4), a two-dimensional Finite Element Model (FEM) is introduced to calculate the effective permeability of the ferrite tile wall with air gaps. Fig. 4 presents the comparison of the two methods. In the analysis, the width of the ferrite tile is taken to be 100mm. The thickness of the ferrite tile is taken to be 6.35mm. Air gaps are assumed to be 0.2mm. Reflectivities for frequencies above 300 MHz are not analyzed using FEM to shorten the CPU time. As shown in Fig.4, the simplified formula (4) demonstrates excellent accuracy as compared to more rigorous full-wave solution.

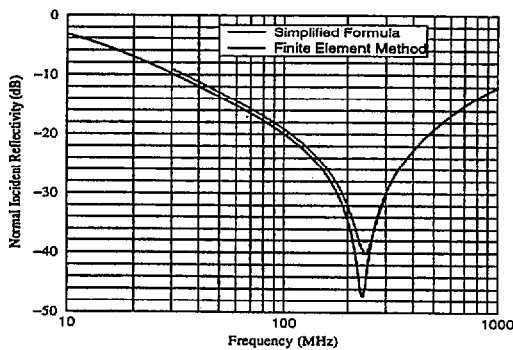


Fig. 4. Comparison of FEM result with simplified air gap model in eqn. (4).

Using the two-dimensional FEM, the staggered ferrite tile installation of the wall is also analyzed. Fig. 5 presents the analysis of staggered tile wall with the same tile and gap dimensions previously stated. As shown in Fig.5, the staggered tile installation regains about 1.7 dB normal incident performance at 30 MHz compared to non-staggered tile installation provided that air gaps between neighboring tiles are the same.

Therefore, staggered ferrite tile wall installation for critical polarization may be implemented to reduce the gap effect given the same installation gap conditions. However, if the staggered installation further widens the air gaps, it may not be worthwhile to implement staggered installation.

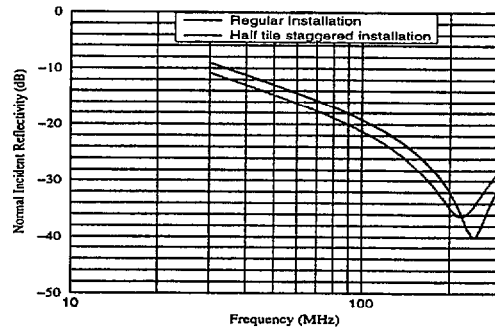


Fig. 5. Analysis of staggered tile installation using finite element method.

(b) **Grid Tiles**-Similar analysis is also performed for grid tiles. It is found that the performance of grid ferrite tile walls is less sensitive to air gaps compared to flat tiles. Fig. 6 shows the analysis the commercial grid tiles having 19mm in tile thickness. The analysis shows that the grid tile can retain a -15dB normal incident reflectivity performance compared to a marginal -10dB from a flat ferrite tile for an assumed averaged 0.2mm air gap between tiles. It is also found that the grid tile has only 50% of the magnetic lossy material active per polarization. Therefore, the grid tile would require twice the volume of sintered ferrite material as flat tile. Due to its grid shape, the effective permeability and permittivity is reduced to less than one third of the bulk material values. This reduced permeability is compensated for by the use of increased thickness to maintain tuning condition at low frequencies. Owing to its reduced permeability, the degradation absorbing properties from air gaps is significantly less than that of the flat tile. Owing to the reduced effective permittivity, the higher frequency performance is extended further. The two added advantages of absorbing performance is gained at the cost of the increased volume of sintered ferrite material.

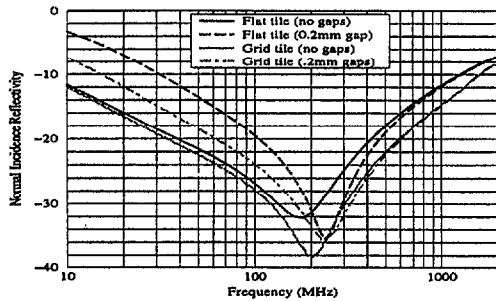


Fig. 6 Comparison of air gap degradation between flat and grid ferrite tiles.

(c). **Hybrid Absorbers**-It becomes apparent that the air gap impact is also very severe to the performance of hybrid absorbers. Without accounting for air gap impact, the design absorber performance will not correspond to the installed wall performance of the EMC chamber. Such a difference will be more significantly observable in an EMC chamber built for 10m test range testing. The air gap degradation of absorber and chamber performance will be very pronounced between 30 and 100 MHz. However, if the gap condition is more severe, EMC chamber performance problem can also be measured above 100 MHz. In order to minimize air gap degradation of the ferrite tiles, the matching foam absorber has to be deep enough to alter the wave impedance before entering the ferrite tile wall so that ferrite tile can still absorb the most significant portion of RF energy from the incident wave at about 30 MHz. For example, hybrid absorbers for a 10m EMC chamber would normally take at least one-meter in total absorber height. Such an absorber height together with the shape of the absorber element is necessary to maintain the transition from low wave impedance region (dielectric absorber region) to high impedance region (magnetic absorber region).

Fig. 7 demonstrates the design and measured performances of EMC Test Systems 1.22m FerroSorb™. It was design with the complex reflection coefficients of ferrite tile panels in a 17m long with 1.84mx1.84m square cross section coax reflectometer. The flat-top matching foam absorber was designed to improve the ferrite tile with a panel installation air gap conditions between ferrite tiles.

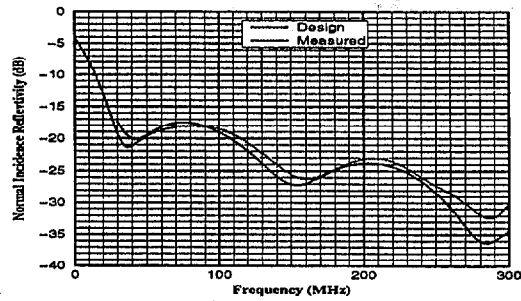


Fig. 7. Design and measured Performance 1.22m FerroSorb™ FS-301.

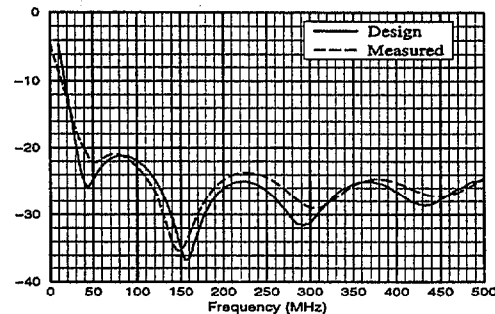


Fig. 8. Design and measured performance of one-meter FerroSorb™ FS-1000.

Fig. 8 presents the comparison of design and measured performance for an improved one-meter FerroSorb™ design with different ferrite tile thickness and shorter foam absorber. A significant enhancement of absorbing performance between 50 and 120 MHz is shown.

The 1.22m FerroSorb™ has been installed in two 10m EMC chambers and successfully meets the FCC site certification testing requirements.

## EMC CHAMBER DESIGN

Having fully characterized the hybrid absorber performance, a computer program was developed based on the multiple-order ray-tracing technique published by Dr. Gavenda to predict the site attenuation performance of EMC chamber.

Fig. 9 shows predicted NSA performance of a 10m EMC chambers in which EMC Test Systems installed its 1.22m FerroSorb™. The Normalized Site Attenuation (NSA) performance is shown for vertical polarization with transmit antenna

positioned at 1m above the floor since the NSA performance for vertical polarization is usually more difficult to achieve. The five NSA curves correspond to measured data taken at the center of the 4m-diameter turntable, 2m front offset, 2m back offset, 2m left offset, and 2m right offset.

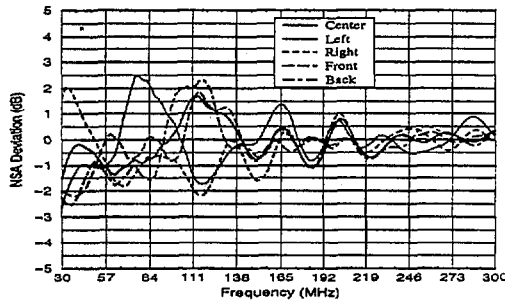


Fig. 9. Predicted NSA deviation from theoretical NSA in an EMC Chamber at 10m test distance.

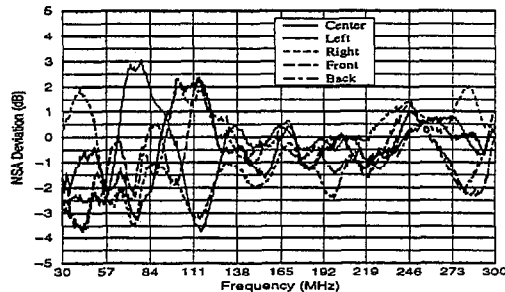


Fig. 10. Measured NSA deviation from theoretical NSA in an EMC chamber at 10m test distance.

Fig. 10 demonstrates the measured NSAs at the corresponding positions. As shown in the two figures, an excellent correlation of NSA performance between predicted and measured has been demonstrated for the 10m test range.

Through our extensive modeling, it is found that the first-order reflection model is inadequate to predict meaningful NSA performance of EMC chamber. Typically, the predicted result will be pessimistic for horizontal polarization, while the result for vertical polarization is grossly optimistic. In order to predict the NSA performance accurately, it is necessary to incorporate up to 4 bounces for sidewalls and endwalls; and 9 bounces for floor and ceiling reflections. Any additional increase of orders in reflection will not result in any notable

improvement in predicted NSA accuracy for EMC chamber design using good absorbers.

It is also found that the predicted NSA data for 3m range distance does not correlate to the measured data as well as that of the 10m range distance even if more reflection order is included in the model.

## CONCLUSIONS

Physical properties of dielectric and ferrite related absorbers have been analyzed and discussed extensively. An empirical formula for ferrite tile performance has been developed and presented for quick evaluation of intrinsic ferrite tile performance at low frequency. A simplified formula for modeling the air gap effect of ferrite tile has been validated for an effective evaluation of EMC absorber walls with ferrite tile installed. Finally, fully characterized hybrid absorber is used to predict the performance of the EMC chamber and shown to correlate to the measured data very well at 10m test range.

## ACKNOWLEDGMENT

The author would like to express his sincere gratitude to Mr. Bryan Saylor Mr. Bobby White for their contribution in facilitating the measurements in large square coax reflectometer.

## References

- [1] K. Liu, and J. M. Kilpela, "Optimized absorber designs for EMC applications," Proc. of 1993 *IEEE Int. Symposium on EMC*, Dallas, TX, USA, pp. 289-292 Aug. 9-13, 1993.
- [2] S. Takeya, and K. Shimada, "New measurement of RF absorber characteristics by large coaxial line," Proc. of 1993 *IEEE Int. Symposium on EMC*, Dallas, TX, USA, pp. 397-402 Aug. 9-13, 1993.
- [3] H. Anzai, Y. Naito, and T. Mizumoto, "Effect of ferrite tiles' gap on ferrite electromagnetic wave absorber," Proc. of 1995 *IEEE Int. Symposium on EMC*, Dallas, TX, USA, pp. 297-302 Aug. 14-18, 1995.
- [4] J. D. Gavenda, "Semi-anechoic chamber site attenuation calculations," Proc. of 1990 *seven Int. Conf. Electrmag. Compat.*, York, UK, pp. 109-113 Aug. 28-31, 1990.